

Effect of Gemini primary mirror position, relative to the lateral support, on mirror figure

M. K. Cho, L. Stepp

Gemini 8m Telescopes Project, 950 N. Cherry Avenue, Tucson, AZ 85719

Gemini Preprint #61

Effect of Gemini primary mirror position, relative to the lateral support, on mirror figure

Myung K. Cho^{a,b}, Larry Stepp^b

^aOptical Sciences Center, University of Arizona, Tucson, AZ 85721

^bGemini 8m Telescopes Project, Tucson, AZ 85726

ABSTRACT

The Gemini primary mirror support incorporates a system of hydraulic whiffletrees to carry the mirror weight and define its position. The six orthogonal kinematic degrees of freedom are controlled by six hydraulic zones -- three axial, two lateral, plus a transverse lateral. By varying the fluid volumes in these hydraulic zones the mirror position can be adjusted in all six degrees of freedom.

Because of the finite lengths of the linkages that connect the mirror to the lateral supports, any shift in mirror position changes the amplitudes and directions of the applied forces with a resulting effect on the static balance and mirror figure. These effects have been calculated for mirror translations and rotations in all six degrees of freedom, resulting in predictions of the changes in the axial and lateral support forces and in the mirror figure. This paper describes the modeling as well as experimental verification of the results.

Key words: lateral support, support force optimization, mirror figure, optical alignment, large telescopes

1. INTRODUCTION

The Gemini primary mirror support system has been described in previous papers and reports ^{1,2,3,4}. The mirror position is defined by a system of hydraulic whiffletrees divided (normally) into six separate zones -- three axial, two lateral, plus a transverse lateral. By varying the fluid volumes in these hydraulic zones the mirror position can be adjusted in all six degrees of freedom. The three axial support zones control piston (Z translation), tip (rotation about X-axis) and tilt (rotation about Y-axis). The two lateral support zones control lateral position (Y translation) and rotation about the optical (Z) axis. The transverse lateral zone controls mirror translation in the X direction. The available range of motion amounts to a few millimeters at the edge of the mirror.

The lateral support system is similar to the Schwesinger ⁵ type of lateral support developed for the ESO VLT. The system has 60 hydraulic support mechanisms attached to the outer edge of the primary mirror with linkages. The orientations of the linkages have been optimized by means of a least squares fit to minimize the change in mirror figure due to changing gravity orientation. As part of this optimization, the resultant of the lateral support forces has been constrained to pass through the center of mass of the mirror.

The lateral support forces are symmetric about the Y axis and antisymmetric about the X axis. This means the orientation of the linkages are mirrored on the upper and lower halves of the mirror, but the lateral supports on the lower (-Y) half push upwards, while the lateral supports on the upper (+Y) half pull upwards. The directions of the lateral support forces are represented as vectors in Figure 1.

In the telescope, the mirror must be adjusted to satisfy optical alignment considerations and proper functioning of the mirror support. The optical axis of the telescope is defined as the rotation axis of the Cassegrain Rotator. This sets the required mirror position in X and Y and its tip-tilt orientation. The working position of the mirror in the Z-direction is partially defined by mechanical considerations. When the mirror is not supported by the axial support system it rests on 120 rubber pads on top of the mirror cell. The working position of the mirror is 3 mm

above this rest position. Rotation of the mirror about the optical axis has no importance optically, but it has some effect on the balance of forces in the support system.

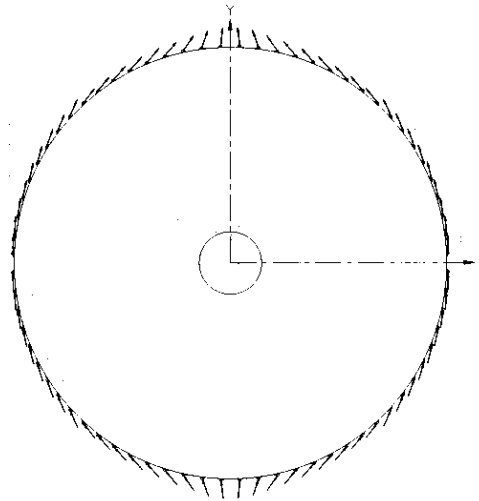


Figure 1. Directions of the forces exerted by the 60 lateral support mechanisms

To achieve these alignment requirements, the position and orientation of the mirror in the six orthogonal directions are measured by LVDTs to a resolution of a fraction of a micron, and controlled by the hydraulic systems to a repeatability of approximately one micron.

After the mirror is installed in the telescope and aligned with the Cassegrain Rotator axis, the lateral support positions must be adjusted to minimize mirror figure change with changing zenith angle, and to ensure that their combined line of action passes through the center of mass of the mirror. The information available to make these adjustments comes primarily from the load cell readings of the axial and lateral supports. For example, when the telescope is horizon pointing the load on the axial supports should read zero and the load on the right half of the lateral supports should equal the load on the left half.

To aid in interpreting the load cell readings, we investigated the effect of small mirror motions in each of the orthogonal degrees of freedom. These case studies are summarized in Table 1.

CASE	DESCRIPTION
1	Translation of 1 mm in +X direction, T_x
2	Translation of 1 mm in +Y direction, T_y
3	Translation of 1 mm in +Z direction, T_z
4	Rotation of 50 arcsec about X-axis, R_x (produces ~1 mm of movement at edge of mirror)
5	Rotation of 50 arcsec about Y-axis, R_y (produces ~1 mm of movement at edge of mirror)
6	Rotation of 50 arcsec about Z-axis, R_z (produces ~1 mm of movement at edge of mirror)

Table 1. Summary of cases studied (rigid body motions in 6 degrees of freedom).

2. CALCULATION OF FORCE AND MOMENT CHANGES

The lateral support linkages are nominally 160 mm long. If the mirror is shifted relative to the lateral support, the orientations of the linkages change and as a result the force exerted by each lateral support is changed in amplitude and direction. For the small movements of which the support system is capable the changes in force amplitude are small and can be neglected, but the changes in direction have a significant effect.

The changes in lateral support forces caused by the six orthogonal movements of the primary mirror have been calculated. For example, for mirror motion parallel to the altitude axis (X translation), the change in lateral forces can be calculated as discussed below.

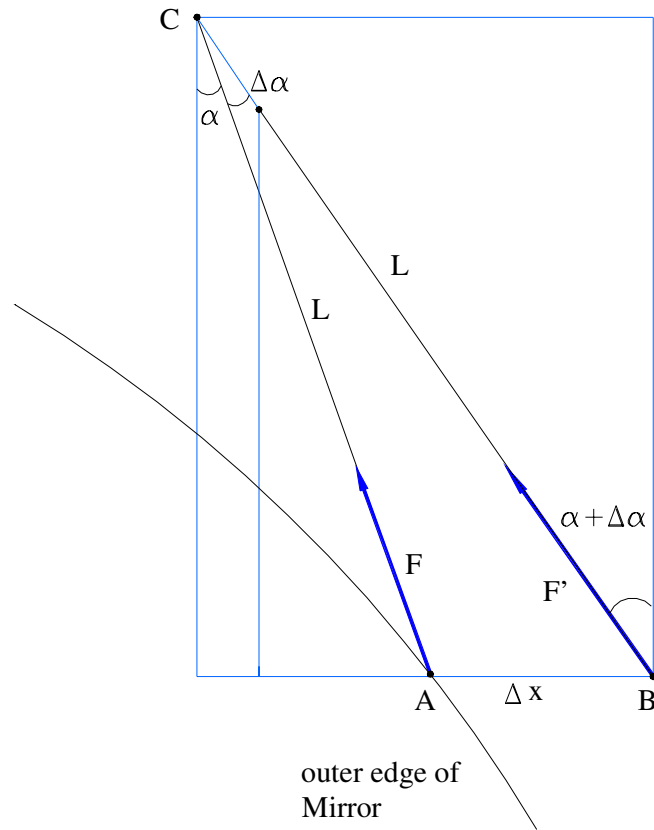


Figure 2. Force variation due to a rigid body translation in the X direction

Figure 2 is a diagram representing one of the lateral support linkages as viewed from above the mirror. In the figure a lateral support linkage of length L connects point A on the edge of the mirror with the lateral support mechanism at C . The force applied by this linkage is denoted as vector F . If the mirror is shifted a distance Dx , the force applied by the linkage is changed to F' , and the angle between the linkage and the Y -axis changes from a to $a + Da$. Since the X translation is small compared to the length of the linkage, the direction of F' is assumed to lie on the line BC . From the geometry with linear infinitesimal assumptions, the X translation can be related to the change in angle as:

$$Dx = L \sin Da / \cos a, \text{ or}$$

$$\sin Da = Dx \cos a / L$$

The magnitude of the resultant force after the translation is assumed to remain unchanged because of the linear infinitesimal assumptions. For a unit translation along the X axis of 1 mm and a linkage length of 160 mm, the changes in the force components at this point are:

$$D F_x = F \sin Da \cos a = F \cos^2 a \, Dx / L = F \cos^2 a / 160$$

$$D F_y = - F \sin Da \sin a = - F \sin a \cos a \, Dx / L = - F \sin a \cos a / 160$$

$$D F_z = F \sin Da \tan b = F \tan b \cos a \, Dx / L = F \tan b \cos a / 160$$

where β is the angle of the force relative to the X-Y plane. This angle is between 0 and 8 degrees, depending on the position on the mirror.

At each end of the linkage is a spherical rod end bearing. The rod end bearings are not frictionless and they can transmit moments when they are loaded by the weight of the mirror. Since the lateral support forces are produced as reactions to the lateral component of the mirror weight, the loads on the linkages increase as the sine of the zenith angle. To avoid creating moments at the linkages, the mirror is raised from its parked position while the telescope is zenith pointing and there is no load on the linkages. Then, it is held in constant position relative to the support system as the telescope changes elevation.

Moments can still be produced if the forces exerted by the lateral support are not aligned with the linkages. Although the lateral support mechanisms have been carefully aligned, a shift in mirror position will change this alignment and induce moments that increase as the sine of the zenith angle. The moments caused by six orthogonal movements of the primary mirror have been calculated. For example, for mirror motion parallel to the optical axis (Z translation), the induced moments on the lateral support linkages can be calculated as discussed

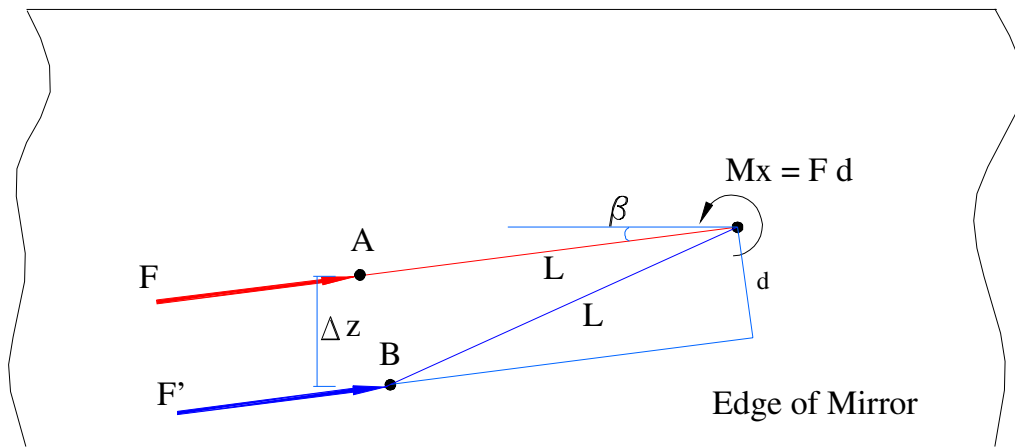


Figure 3. Moment due to a rigid body translation in the Z direction

below.

Figure 3 is a diagram representing one of the lateral support linkages as viewed from the side of the mirror, that is, looking in the $-X$ direction. The force F is applied by the lateral support mechanism at point A through the linkage L , and the force is initially aligned with the linkage. If the mirror is raised a distance Dz , the relative position of the lateral support mechanism shifts to point B. The force is no longer aligned with the linkage, so if the telescope is tilted away from the zenith a moment is produced:

$$M = F d = F Dz \cos b$$

The components are:

$$M_x = F Dz \cos b \cos a$$

$$M_y = F Dz \cos b \sin a$$

The net force and moment changes due to the six degrees of freedom have been calculated and are listed in Table 2. The principal resultant forces and moments are shown, with an indication of which load cell readings will be affected. These values are for horizon-pointing (zenith angle 90 degrees). The effects at other zenith angles will be in proportion to the sine of the zenith angle.

As can be seen from Table 2, in only two cases do the moments caused by friction in the rod ends have an effect on the overall force or moment applied to the mirror. In both these cases, the moments work in opposition to the effect of the change in direction of the forces, with a smaller amplitude.

Mirror Motion	Amplitude (all in positive direction)	Effect on Global Force Balance		
		Amplitude and direction		Load Cells Affected
		Effects of Forces	Effects of Moments	
CASE 1, T_x	+ 1 mm	3100 N-m moment about Z-axis	- 222 N-m moment about Z-axis	Lateral
CASE 2, T_y	+ 1 mm	————	————	
CASE 3, T_z	+ 1 mm	- 3100 N-m moment about X axis	230 N-m moment about X axis	Axial
CASE 4, R_x	50 arcsec (1 mm at edge of mirror)	- 770 N force in Z direction	————	Axial
CASE 5, R_y	50 arcsec (1 mm at edge of mirror)	————	————	
CASE 6, R_z	50 arcsec 1 mm at edge of mirror	770 N force in X direction	————	X-definer

Table 2. Effect of mirror movement, relative to lateral support system, on global support forces and moments

Note that the lateral forces and moments caused by mirror motions can disturb the static force equilibrium state. For example, CASE 3 (Z translation) causes the resultant of the lateral support forces to no longer pass through the center of gravity. As a result, the mirror will tend to rotate about the X-axis, causing uneven loading of the axial support system. CASE 4 (X rotation) causes the lateral support forces to exert a net force in the Z direction. As a result, the mirror will push against or lift off from the axial supports, depending on the direction of rotation.

3. FINITE ELEMENT ANALYSES

3.1 Finite element model

A finite element model of the primary mirror was developed to evaluate the optical surface distortion. Around the edge of the mirror, the 60 lateral support attachment blocks were modeled by elements with equivalent stiffness and weight. The model consists of 2568 thin shell elements and 2508 nodes using I-DEASTM software⁶.

In order to simulate the behavior of the mirror precisely, multiple point constraint (MPC) condition features were incorporated in the finite element model. These features provide a good simulation of the properties of the hydraulic whiffletree systems described in previous sections. Six MPC conditions were applied to the mirror model – three for the axial support zones, two for lateral support zones, and one for the transverse lateral direction.

3.2. Analysis results

For each of the six cases described above, the effects of the lateral force changes to the optical surface figure at horizon pointing were evaluated using the finite element model. The optical surface figure maps for the six rigid body cases are shown in Figure 4. Table 3 gives the results in terms of RMS surface errors, after removing piston, tilt, and focus terms, and characterizes the changes in terms of the coefficients of the major Zernike polynomial terms. Blanks in the table represent coefficients less than 0.01 microns. In all six cases, higher order Zernike terms were at least an order of magnitude smaller than the terms listed in the table.

The horizon-pointing optical surface figures caused by the rod end applied moments was also evaluated. The figure maps for the six rigid body cases are shown in Figure 5. The same contour interval as in Figure 4 was used to illustrate the relative magnitude of optical surface distortions. Table 4 gives the results in terms of RMS surface errors, after removing piston, tilt, and focus terms, and characterizes the figure changes in terms of the coefficients of the major Zernike polynomial terms.

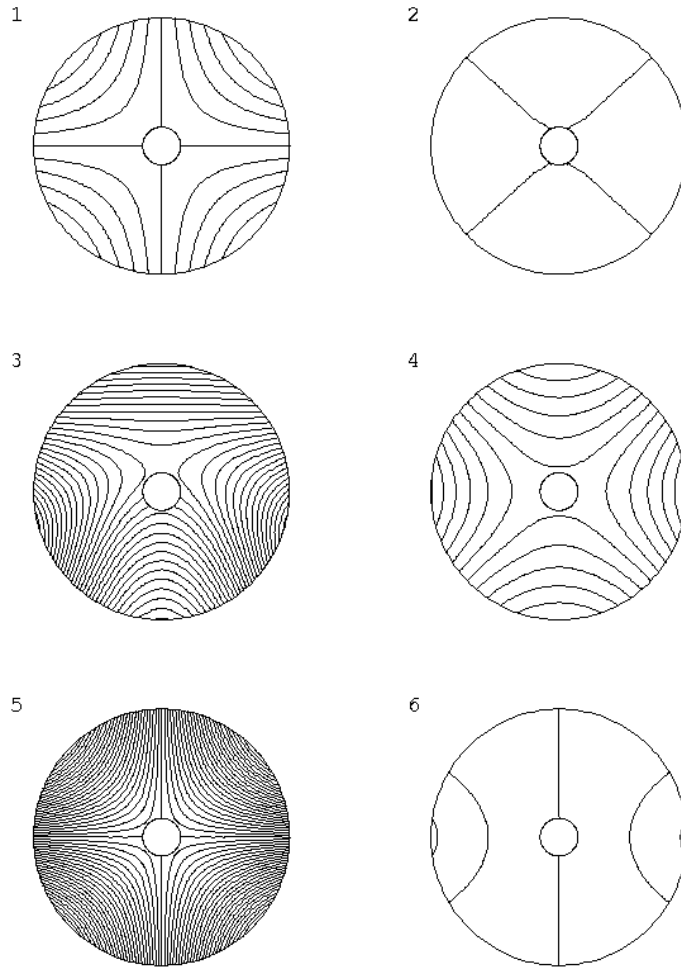


Figure 4. Optical surface figures caused by forces from 1 mm mirror motions in each of the six degrees of freedom, at horizon pointing (contour interval = 0.5 microns).

Mirror Motion	Optical Surface RMS (microns)	Principal Effects on Mirror Figure Zernike Polynomial Coefficients (microns)					
		0 Astig	45 Astig	0 Coma	90 Coma	0 Trefoil	30 Trefoil
CASE 1, T_x	1.08		2.49				
CASE 2, T_y	0.18	-0.42					
CASE 3, T_z	2.95	6.41			-1.44		-2.26
CASE 4, R_x	1.20	2.77					
CASE 5, R_y	5.50		12.70				
CASE 6, R_z	0.15			0.12		0.35	

Table 3. Calculated effects of forces from 1 mm mirror motions in each of the six degrees of freedom, at horizon pointing.

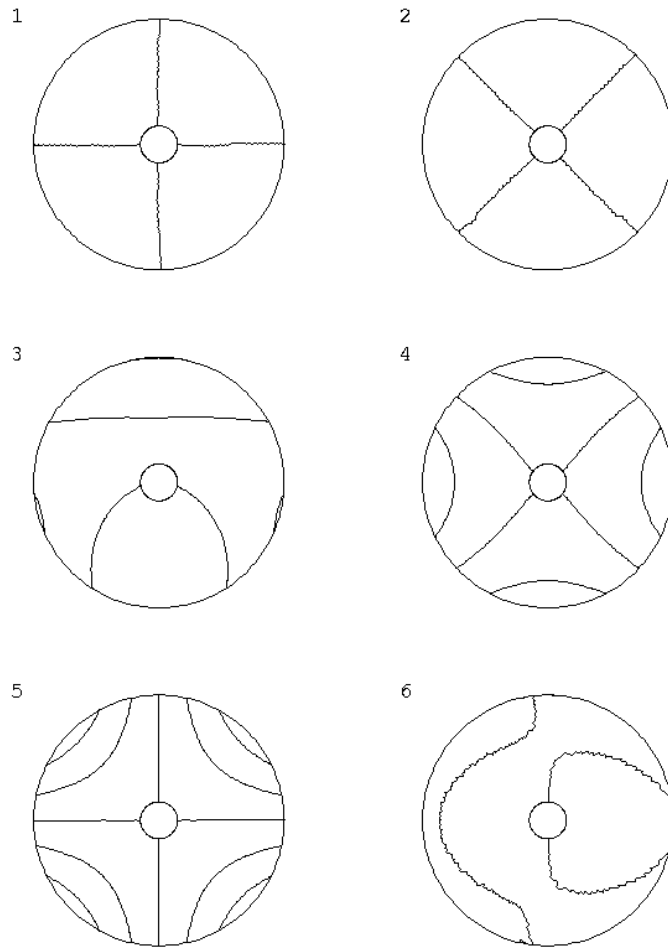


Figure 5. Optical surface figures caused by rod end moments from 1 mm mirror motions in each of the six degrees of freedom, at horizon pointing (contour interval = 0.5 microns).

Mirror Motion	Optical Surface RMS (microns)	Principal Effects on Mirror Figure Zernike Coefficients (microns)					
		0 Astig	45 Astig	0 Coma	90 Coma	0 Trefoil	30 Trefoil
CASE 1, T_x	0.05		-0.12				
CASE 2, T_y	0.03	0.07					
CASE 3, T_z	0.22	-0.46			0.21		
CASE 4, R_x	0.36	-0.83				0.01	
CASE 5, R_y	0.52		-1.20				
CASE 6, R_z	0.01			-0.01			0.01

Table 4. Calculated effects of rod end moments from 1 mm mirror motions in each of the six degrees of freedom, at horizon pointing.

Note that these results represent the amount of additional mirror figure change that will occur when going from zenith to the horizon if the mirror has been moved by the amount indicated. The RMS values can be compared to the calculated zenith-horizon figure change with the nominal lateral support, which is 0.28 micron RMS before active optics correction.

The effects in each case are almost entirely astigmatism, coma and trefoil. The astigmatism and trefoil can be readily corrected by the active mirror support and the coma can be corrected by adjusting the position of the secondary, but it is better to minimize these effects by proper alignment of the lateral support system, to reduce the active optics requirements. The largest effects are produced by rotation about the Y-axis and translation along the Z-axis. In the telescope, these effects have been corrected by shimming of the lateral supports.

In operation, a look-up table will define the nominal mirror support forces to be applied as a function of zenith angle. It can be seen from Table 2 that it is important to align the primary mirror in the telescope before developing the look-up table. Once the mirror position is established, motions of one or two microns during operation of the telescope will have negligible effect on the optical surface for any of these cases.

One other case has been investigated – uniform thermal expansion of the mirror cell relative to the mirror. The effects of a 1 mm increase in the diameter of the mirror cell, corresponding to a temperature increase of about 12 degrees C, are negligible.

4. EMPIRICAL MEASUREMENTS

During integration of the Mauna Kea Gemini Telescope a number of tests were performed to evaluate and adjust the mirror support system. For these tests the secondary mirror assembly was replaced by a prime focus wavefront sensor. Several of the tests provided confirmation of the calculations described above.

During the tests data were recorded by the primary control system (PCS). The PCS measures the position and orientation of the mirror in six orthogonal degrees of freedom, as well as loadcell readings at the 120 axial supports, the 60 lateral supports, and at 4 of the transverse lateral actuators that we call X-definers. These readings are recorded along with the zenith angle and information about the wavefront measurements.

4.1. Determining the optimum position in Z

If the lateral supports are not at the correct height relative to the mirror, relatively large moments are produced about the X-axis and the mirror will change figure between zenith and horizon. This is quantified as Case 3 in Figure 4 and Tables 2, 3, and 4, above. After the mirror had been aligned to the Cassegrain Rotator axis and its height set relative to the rubber rest pads, we performed an elevation test to determine the position of the mirror relative to the lateral support system. Throughout the test the PCS kept the mirror in its correct operating position relative to the mirror cell.

Load cell readings were recorded at several different zenith angles. The test started with the telescope at the zenith and readings were taken at increments of five degrees from the zenith to the horizon. From the load cell readings the total moment about the X-axis (M_x) was calculated. This is plotted as a function of zenith angle in Figure 6.

The goal is to have the support system exert no net moment about the X-axis at any elevation angle. However, the moment is not zero even at the zenith. Examination of the data indicates this was caused primarily by zero-offset errors in the load cells. Therefore, the immediate goal was to minimize the change in moment about the X-axis as a function of zenith angle.

A sine function and constant term were fit to the data; the amplitude of the change from zero to horizon was about 7575 N-m. The required global shim height adjustment was determined by dividing the 7575 N-m moment by the

calculated value of 3100 N-m per millimeter, which indicated the shims should be increased in height by 2.4 mm. This calculation neglected the smaller effect of moments at the linkage joints.

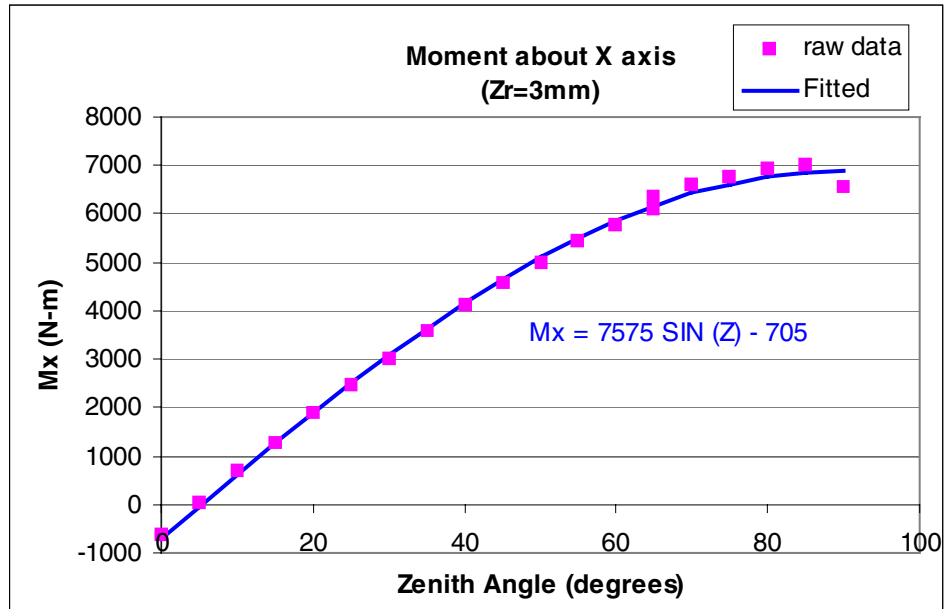


Figure 6. Moment about the X-axis as a function of zenith angle, for the original lateral support shim

The shims under the lateral supports and X-definers were increased by 2.4 mm. We were careful to keep the line of action of each actuator piston parallel to the linkage, and the support mechanisms have now been match drilled and pinned to fix this alignment.

The mirror cell was reinstalled in the telescope and the elevation test was repeated. These measurements are shown in Figure 7. The change in moment as a function of zenith angle was reduced by two orders of magnitude.

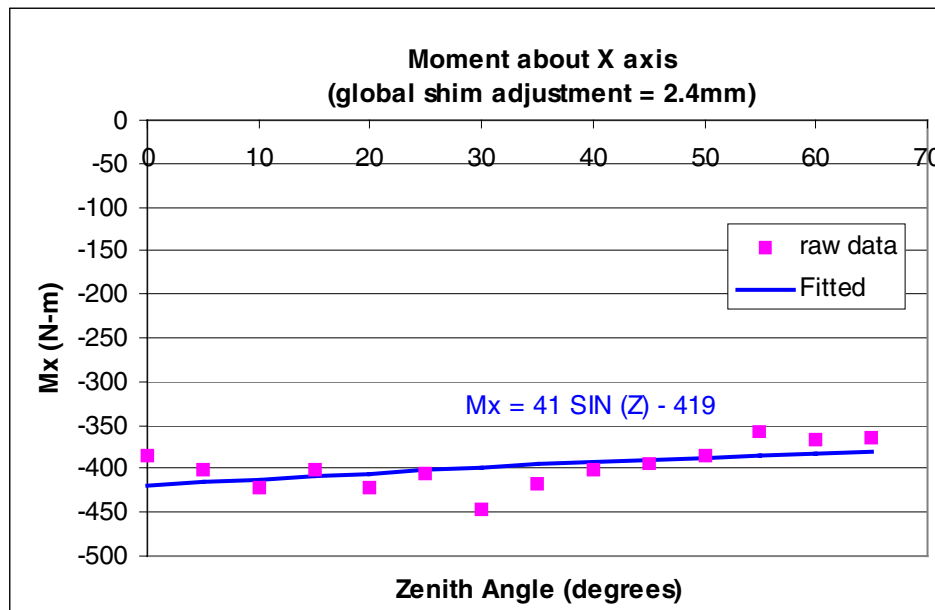


Figure 7. Moment about the X-axis as a function of zenith angle after the global shim adjustment of + 2.4

During these tests we also demonstrated the moment about the Y axis (M_y) was insensitive to the zenith angle.

4.2. Confirmation of mirror figure changes caused by rigid body motion

Several tests were run where the mirror figure was measured as a function of zenith angle, without changing the forces exerted by the axial supports. By comparing tests performed with the mirror in different positions, we can confirm the effect of mirror position on mirror figure.

In each test, the mirror figure was measured by the prime focus wavefront sensor (PFWFS) using WaveLab™ software. At the start of the test the mirror figure was optimized with the telescope tracking a star near the zenith. The telescope was then pointed to a star approximately 15 degrees from the zenith, without changing the active forces, and the figure was remeasured. This was repeated at intervals of approximately 15 degrees to a zenith angle of greater than 60 degrees, then back by 15 degree intervals to the zenith. At each star, the mirror figure was measured three times. The mirror figure data was evaluated in terms of Zernike coefficients. Then, for several of the low-order Zernike terms the measurements were fit to a sine function of zenith angle.

Table 5 gives the results for tests run on several nights in October, 1999. On October 22 the mirror was in its nominal, aligned position. On October 27, the mirror had been tilted +125 microradians about the X-axis and +185 microradians about the Y-axis. On October 29, the mirror tilt remained the same but the mirror was moved -1 mm in the Z direction. For each test the measured values of each Zernike coefficient were fit to a sine function plus a constant term.

Zernike Term	Results of sine fit: $f(z) = m \sin(z) + b$					
	Test on October 22		Test on October 27		Test on October 29	
	M	b	m	b	m	b
0 Astig	0.32	-1.26	1.82	-2.31	-9.271	2.905
45 Astig	-15.37	2.35	-5.33	0.29	-6.516	0.238
0 Coma	1.45	-0.50	1.69	0.08	1.381	-0.101
90 Coma	0.09	0.02	0.29	0.22	2.241	-0.274
Spherical	-0.03	-0.17	0.01	-0.13	0.104	-0.282
0 Trefoil	-0.71	0.14	-0.72	0.22	-1.707	0.452
30 Trefoil	-0.79	0.56	-0.79	0.22	2.257	1.801

Table 5. Coefficients and intercepts of sine functions fit to mirror figure data. Values are in microns.

Table 6 compares the mirror figure changes predicted by the values in Table 2 to the changes actually measured. In both cases, the changes in the Zernike coefficients occurred as predicted. The amplitudes match quite well in the first case and fairly well in the second case. The test on the night of October 29 was interrupted by clouds and only a few data points were taken, which limited the accuracy of the sine fits.

Zernike Term	Comparisons between predicted & measured change in coefficients			
	October 22 to October 27		October 27 to October 29	
	D m (predicted)	D m (measured)	D m (predicted)	D m (measured)
0 Astig	1.42	1.50	-6.41	-11.09
45 Astig	9.63	10.03	0.00	-1.18
0 Coma	0.00	0.24	0.00	-0.31
90 Coma	0.00	0.20	1.44	1.96
Spherical	0.00	0.04	0.00	0.09
0 Trefoil	0.00	-0.01	0.00	-0.99
30 Trefoil	0.00	-0.00	2.26	3.04

Table 6. Comparison of predicted and measured changes in sine fit coefficients. Values are in microns.

5. SUMMARY AND CONCLUSIONS

With the Schwesinger type of lateral support used by Gemini, changes in mirror position and orientation relative to the lateral support mechanisms affect the directions of the applied forces, which in turn affects the way the mirror figure changes with zenith angle. We have calculated the changes in forces and moments due to mirror movements in each of the six orthogonal degrees of freedom. The resulting information guided our adjustments of the height of the Gemini lateral supports. We were able to reduce the change in moment about the X-axis as a function of zenith angle by two orders of magnitude.

The effects of these forces and moments on the mirror figure were also calculated. The effects of the moments are small compared to the effects of the changing force directions. Mirror motion produces almost entirely astigmatism, coma and trefoil; therefore, the effects can be readily corrected by active optics, if necessary.

Tests performed with a prime focus wavefront sensor verified that the measured figure changes are in good agreement with the predicted values.

There are two other lessons to be learned from this study:

- Because small motions of the mirror can cause relatively large figure changes, the final alignment of the mirror should be set before building look-up tables for open-loop active optics figure control.
- Because the linkage rod end bearings are not frictionless, the mirror should always be placed in its operating position while the telescope is zenith pointing, to avoid unpredictable figure changes caused by stick-slip at the linkages.

ACKNOWLEDGEMENT

This research was funded by the Gemini 8-m Telescopes Project. The Gemini 8-m Telescopes Project and observatory is managed by the Association of Universities for Research in Astronomy, for the National Science Foundation and the Gemini Board, under an international partnership agreement.

REFERENCES

1. L. Stepp, E. Huang and M. Cho, "Gemini primary mirror support system", *Advanced Technology Optical Telescopes V*, ed. L. Stepp, vol. 2199, pp. 223-238, SPIE, Kona, 1994.
2. M.K. Cho and R. S. Price, "Optimization of Support Point Locations and Force Levels of the Primary Mirror Support System", Gemini Project technical report RPT-O-G0017, November 5, 1993.
3. L. Stepp and M. Cho, "The Distributed Defining System for the Primary Mirror", RPT-O-G0023, November 1993.
4. M.K. Cho and R.S. Price, "Theoretical Active Optics Performance of the Gemini 8-M Primary Mirror", Gemini Project technical report RPT-O-G0032, November 1993.
5. G. Schwesinger, "Lateral support of very large telescope mirrors by edge forces only", *Journal of Modern Optics*, Vol. 38, No. 8, pp. 1507-1516, 1991.
6. Mark H. Lawry, "I-DEAS Master Series", Structural Dynamics Research Corporation, Millford, OH., 1997.